Journal of Sound and Vibration (2000) **233**(5), 857–875
doi:10.1006/jsvi.1999.2855, available online at http://www.idealibrary.com on IDEAL®

FREE VIBRATION OF CENTRIFUGALLY STIFFENED UNIFORM AND TAPERED BEAMS USING THE DYNAMIC STIFFNESS METHOD

J. R. BANERJEE

Department of Mechanical Engineering and Aeronautics, City University, Northampton Square, London ECIV OHB, England. E-mail: j.r.banerjee@city.ac.uk

(*Received* 9 *April* 1999, *and in final form* 2 *December* 1999)

Starting from the governing differential equations of motion in free vibration, the dynamic stiffness matrix of a uniform rotating Bernoulli–Euler beam is derived using the Frobenius method of solution in power series. The derivation includes the presence of an axial force at the outboard end of the beam in addition to the existence of the usual centrifugal force arising from the rotational motion. This makes the general assembly of dynamic stiffness matrices of several elements possible so that a non-uniform (or tapered) rotating beam can be analyzed for its free-vibration characteristics by idealizing it as an assemblage of many uniform rotating beams. The application of the derived dynamic stiffness matrix is demonstrated by investigating the free-vibration characteristics of uniform and non-uniform (tapered) rotating beams with particular reference to the Wittrick–Williams algorithm. The results from the present theory are compared with published results. It is shown that the proposed dynamic stiffness method offers an accurate and effective method of free-vibration analysis of rotating beams.

1. INTRODUCTION

Using traditional methods that are based on the derivation of differential equations and application of boundary conditions, the free-vibration characteristics of uniform rotating Bernoulli–Euler beams have been studied by a number of investigators [1–4]. Some of these investigators have emphasized the practical importance of such studies with illustrative examples of engineering applications, for example, see Figure 3 reference [3]. Other investigators have focused their attention solely on rotating cantilever beams [5–7] because turbine, propeller and helicopter blades are sometimes idealized as cantilever beams. During the historical development of this subject, a number of solution techniques with varying degrees of applicability have been suggested in the literature. The Southwell principle [8], the Rayleigh–Ritz method [9], the perturbation technique [10], the method of integral equations [11] and Galerkin method [12] are some examples which need special mention. Most of these investigations are confined to the free-vibration analysis of a single rotating structural (beam) element although there are however, some notable exceptions where finite element-based procedures [13–16] which extend the generality of applications to cover non-uniform distribution of structural properties have been discussed. Other contributors in this field include Stafford and Giurgiutiu [17] and Giurgiutiu and Stafford [18], who have used a semi-analytic approach by employing a transfer matrix formulation in terms of the beam functions, which are essentially the series solutions of the governing differential equations.

An alternative powerful and elegant method of free-vibration analysis is to use the method of the dynamic stiffness matrix [19]. Indeed the method has been used quite extensively for non-rotating beams and there is a wealth of literature on the subject [20, 21]. It appears that no one has used the dynamic stiffness method to investigate the free-vibration characteristics of rotating beams. A survey by the author shows that there is a gap in the literature in this respect. The central purpose of this paper is to fill this gap and extend the elegance of the dynamic stiffness method to the simple case of a uniform rotating Bernoulli–Euler beam as a novel preliminary step. This useful extension of the dynamic stiffness method even to the simple case of a Bernoulli–Euler beam is far from trivial. Indeed as it will be seen later, considerable analytical and computational efforts are required to derive the dynamic stiffness matrix of a rotating Bernoulli–Euler beam. Starting from the basic governing differential equations in free vibration, the dynamics stiffness matrix of a uniform rotating Bernoulli–Euler beam is derived in this paper with the effects of hub radius and a constant concentrated axial force at the outboard end of the beam taken into account. The derived dynamic stiffness matrix is applied with particular reference to a well-known algorithm [22] to solve the free-vibration problem of a few but carefully chosen uniform and non-uniform rotating beams for which some comparative results are available [1, 3, 14]. The research reported in this paper is expected to pave the way for further research on the dynamic stiffness formulation of complex rotating systems.

In view of the smallness of the dynamic stiffness literature in sharp contrast to the massive finite element literature available to date, the following comments are relevant.

Unlike the finite element method in which the mass and stiffness matrices of a structural element are obtained separately, the dynamic stiffness method involves only one frequency-dependent matrix called the dynamic stiffness matrix which contains both the mass and stiffness properties of the structural element. Another important but related difference between the two methods is that the finite element method uses an approximate shape function of the structural element whereas the shape function used in the dynamic stiffness method is exact, and is generally obtained from the analytical solution of the governing differential equation of motion of the structural element. Thus, the finite element method accounts for a finite number of degrees of freedom of a structure (or a structural element). By contrast, the dynamic stiffness method accounts for an infinite number of degrees of freedom of a vibrating structure (or a structural element). Naturally, the accuracy of results in the finite element method is dependent upon the number of elements used and hence the number of degrees of freedom chosen, and estimates of higher order natural frequencies in free-vibration problems are considerably less accurate than the lower order ones. On the other hand, the dynamic stiffness method has no such limitations and the results are independent of the number of elements used in the analysis. For instance, a single element can be used to calculate any number of "exact" natural frequencies and modes of a structure to any desirable accuracy. The assembly procedure for adding element matrices to obtain the overall master matrix of the final structure is essentially the same for both methods. However, the solution techniques can be quite different in the sense that the finite element method generally leads to a linear eigenvalue problem whereas the dynamic stiffness method often leads to a (non-linear) transcendental eigenvalue problem.

2. THEORY

Figure 1 shows the axis system of a typical Bernoulli–Euler beam element of length L with its left-hand end at a distance r_i from the axis of rotation. Note that r_i may or may

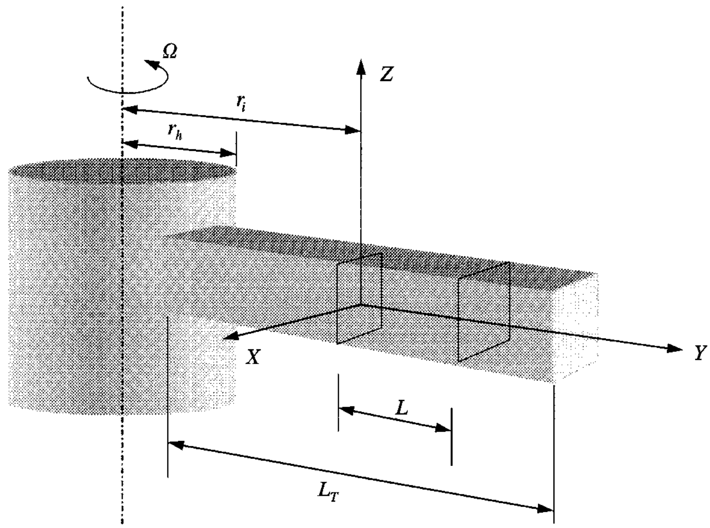

Figure 1. Co-ordinate system and notation for a rotating Bernoulli–Euler beam.

not be equal to the hub radius r_h, and also L may or may not be equal to the total length L_T shown in the figure. The beam is assumed to be rotating at a constant angular velocity Ω and has a doubly symmetric cross-section such as a rectangle or a circle so that the bending and torsional motions as well as the in-plane and out-of-plane motions are uncoupled. In the right-handed Cartesian co-ordinate system chosen, the origin is taken to be at the left-hand end of the beam as shown—the Y-axis coinciding with the neutral axis of the beam in the undeflected position. The Z-axis is taken to be parallel (but not coincidental) with the axis of rotation while the X-axis lies in the plane of rotation. The principal axes of the beam cross-section are, therefore, parallel to X and Z directions. The system is able to flex in the Z direction (flapping) and in the X direction (lead-lag motion). These two motions can be coupled only through Coriolis forces, but for the system shown for the present analysis, this coupling is ignored.

The dynamic stiffness development which follows concerns the out-of-plane free vibration of the beam so that the displacements are confined only in the YZ-plane as shown in Figure 2(a). (It will be explained later that the dynamic stiffness matrix for the in-plane motion of the beam can be derived from the out-of-plane case by suitable substitutions of parameters relating to the rotational speed and the bending rigidity of the beam in the corresponding plane.) The beam element is assumed to be undergoing free natural vibration with circular (angular) frequency ω in the YZ-plane, but has an outboard force F which may arise as a result of the centrifugal force experienced by an adjacent element. The inclusion of this force F allows a general applicability of the method so that the derived dynamic stiffness matrix can be assembled to study the free-vibration characteristics of a beam with a complex geometry and non-uniform distribution of structural properties. Of course, the outboard force F needs to be calculated for each elemental segment representing the beam by using the expression for centrifugal force, see equation (1) below, and noting that this force is zero at the free (tip) end of the beam.

In order to derive the equilibrium equations the forces acting on an incremental length $\mathrm{d}y$ at an instant of time t are shown in Figure 2(b). The senses shown for these forces constitute a positive sign definition in this paper for axial force (T), bending moment (M) and shear force (V) respectively.

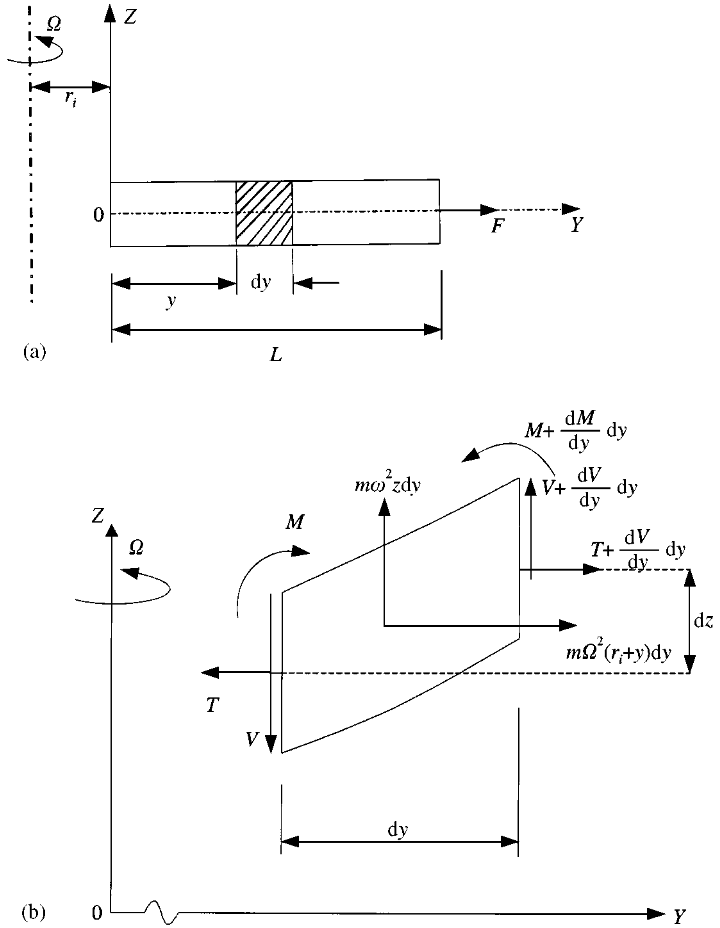

Figure 2. (a) Out-of-plane vibration of a rotating beam element of length L. (b) The forces acting on an incremental element dy during out-of-plane vibration.

The governing differential equations of motion of the beam element can now be derived using Newton's second law by considering the equilibrium of the infinitesimal length dy of the beam element shown in Figure 2(b).

Referring to Figure 2(a), the centrifugal tension $T(y)$ at a distance y from the origin with the inclusion of an outboard force F is given by [3]

$$T(y) = 0{\cdot}5m\Omega^2(L^2 + 2Lr_i - 2r_iy - y^2) + F, \tag{1}$$

where m is the mass per unit length of the beam and Ω is the rotational speed in radian per second.

Consideration of equilibrium of an infinitesimal element shown in Figure 2(b) in the Y and Z directions gives

$$\frac{\mathrm{d}T}{\mathrm{d}y} + m\Omega^2(r_i + y) = 0 \tag{2}$$

and

$$\frac{\mathrm{d}V}{\mathrm{d}y} + m\omega^2 z(y) = 0. \tag{3}$$

Finally, rotational equilibrium of the element about the X-axis gives

$$V + \frac{\mathrm{d}M}{\mathrm{d}y} - T(y)\frac{\mathrm{d}z}{\mathrm{d}y} = 0. \tag{4}$$

The Bernoulli–Euler bending moment equation is given by

$$M(y) = EI_{xx}\frac{\mathrm{d}^2 z}{\mathrm{d}y^2}, \tag{5}$$

where E is the Young's modulus of the beam material and I_{xx} is the second moment of area of the cross-section about the X-axis so that EI_{xx} is the flexural rigidity of the beam in the YZ plane.

Equations (1)–(5) can be combined into one differential equation and can be expressed in non-dimensional form as follows:

$$\mathrm{D}^4\bar{h}(\xi) - \{0{\cdot}5v^2(1 + 2\rho_0 - 2\rho_0\xi - \xi^2) + \eta\}\mathrm{D}^2\bar{h}(\xi) + v^2(\rho_0 + \xi)\mathrm{D}\bar{h}(\xi) - \mu^2\bar{h}(\xi) = 0, \tag{6}$$

where

$$\mathrm{D} = \mathrm{d}/\mathrm{d}\xi, \qquad \xi = y/L, \qquad \bar{h}(\xi) = z/L, \qquad \rho_0 = r_i/L, \qquad \mu^2 = m\omega^2 L^4/EI_{xx},$$

$$v^2 = m\Omega^2 L^4/EI_{xx}, \qquad \eta = FL^2/EI_{xx}. \tag{7}$$

Thus, the dimensionless expressions for tension, bending moment and shear force are defined as

$$\beta(\xi) = T(y)L^2/EI_{xx} = 0{\cdot}5v^2(1 + 2\rho_0 - 2\rho_0\xi - \xi^2) + \eta,$$

$$\bar{M}(\xi) = M(y)L/EI_{xx}, \qquad \bar{V}(\xi) = V(y)L^2/EI_{xx}. \tag{8}$$

Equation (6) is a linear ordinary differential equation with variable coefficients and is, therefore, amenable to power series solution in terms of the independent variable ξ. Using the Frobenius method, the solution is sought in the form of the following series [1, 3]:

$$f(\xi, k) = \sum_{n=0}^{\infty} a_{n+1}(k)\xi^{k+n}, \tag{9}$$

where a_{n+1} are the coefficients and k is an undetermined exponent.

Substituting equation (9) into equation (6), one obtains the following indicial equation [1, 3]:

$$k(k-1)(k-2)(k-3) = 0 \tag{10}$$

and the following recurrence relationship [1, 3]:

$$a_{n+5}(k) = \frac{\{0{\cdot}5v^2(1+2\rho_0)+\eta\}}{(k+n+4)(k+n+3)}\,a_{n+3}(k) - \frac{v^2\rho_0(k+n+1)}{(k+n+4)(k+n+3)(k+n+2)}\,a_{n+2}(k)$$
$$-\frac{0{\cdot}5v^2(k+n)(k+n+1)-\mu^2}{(k+n+4)(k+n+3)(k+n+2)(k+n+1)}\,a_{n+1}(k), \tag{11}$$

where the first four coefficients are defined as

$$a_1(k)=1,\quad a_2(k)=0,\quad a_3(k)=\frac{\{0{\cdot}5v^2(1+2\rho_0)+\eta\}}{(k+2)(k+1)},\quad a_4(k)=-\frac{v^2\rho_0 k}{(k+3)(k+2)(k+1)}. \tag{12}$$

The roots of the indicial equation (10) are $k = 0$, 1, 2 and 3 so that the four linearly independent solution functions $f(\xi, 0)$, $f(\xi, 1)$, $f(\xi, 2)$ and $f(\xi, 3)$ are given by

$$f(\xi,0) = 1 + \{0{\cdot}5v^2(1+2\rho_0)+\eta\}\xi^2/2 + \sum_{n=0}^{\infty} a_{n+5}(0)\xi^{n+4}, \tag{13}$$

$$f(\xi,1) = \xi + \{0{\cdot}5v^2(1+2\rho_0)+\eta\}\xi^3/6 - v^2\rho_0\xi^4/24 + \sum_{n=0}^{\infty} a_{n+5}(1)\xi^{n+5}, \tag{14}$$

$$f(\xi,2) = \xi^2 + \{0{\cdot}5v^2(1+2\rho_0)+\eta\}\xi^4/12 - v^2\rho_0\xi^5/30 + \sum_{n=0}^{\infty} a_{n+5}(2)\xi^{n+6}, \tag{15}$$

and

$$f(\xi,3) = \xi^3 + \{0{\cdot}5v^2(1+2\rho_0)+\eta\}\xi^5/20 - v^2\rho_0\xi^6/40 + \sum_{n=0}^{\infty} a_{n+5}(3)\xi^{n+7}. \tag{16}$$

Hence, the general solution of the differential equation (6) may be written as

$$\bar{h}(\xi) = C_1 f(\xi,0) + C_2 f(\xi,1) + C_3 f(\xi,2) + C_4 f(\xi,3), \tag{17}$$

where C_1, C_2, C_3 and C_4 are four arbitrary constants.

Using the sign convention of Figure 2(b) to be all positive, the expressions for the anti-clockwise (tangential) rotation or beam slope ($\bar{\theta}$), bending moment ($\bar{M}$) and shear force ($\bar{V}$) are, respectively, given in non-dimensional forms as follows (see equation (8)):

$$\bar{\theta}(\xi) = \bar{h}'(\xi) = C_1 f'(\xi,0) + C_2 f'(\xi,1) + C_3 f'(\xi,2) + C_4 f'(\xi,3), \tag{18}$$

$$\bar{M}(\xi) = \bar{h}''(\xi) = C_1 f''(\xi,0) + C_2 f''(\xi,1) + C_3 f''(\xi,2) + C_4 f''(\xi,3) \tag{19}$$

and

$$\begin{aligned}\bar{V}(\xi) &= -\bar{h}'''(\xi) + \beta(\xi)\bar{h}'(\xi)\\ &= -\{C_1 f'''(\xi,0) + C_2 f'''(\xi,1) + C_3 f'''(\xi,2) + C_4 f'''(\xi,3)\}\\ &\quad + \beta(\xi)\{C_1 f'(\xi,0) + C_2 f'(\xi,1) + C_3 f'(\xi,2) + C_4 f'(\xi,3)\},\end{aligned} \tag{20}$$

where a prime denotes differentiation with respect to ξ.

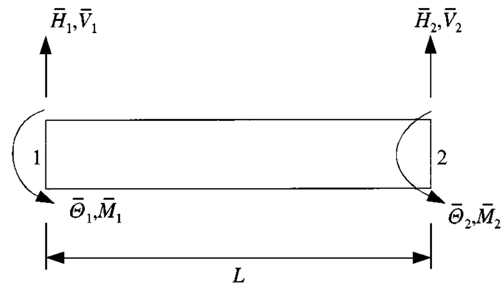

Figure 3. End conditions for displacements and forces of the beam element.

The dynamic stiffness matrix which relates the amplitudes of harmonically varying forces to the corresponding harmonically varying displacement amplitudes at the ends of the element, can now be derived by imposing the end conditions for displacements and forces.

The end conditions for displacements and forces of the element (see Figure 3) are, respectively,

Displacements:

$$\text{at end 1 } (\xi = 0)\text{: } \bar{h} = \bar{H}_1, \quad \bar{\theta} = \bar{\Theta}_1, \tag{21}$$

$$\text{at end 2 } (\xi = 1)\text{: } \bar{h} = \bar{H}_2, \quad \bar{\theta} = \bar{\Theta}_2. \tag{22}$$

Forces:

$$\text{at end 1 } (\xi = 0)\text{: } \bar{V} = -\bar{V}_1, \quad \bar{M} = -\bar{M}_1, \tag{23}$$

$$\text{at end 2 } (\xi = 1)\text{: } \bar{V} = \bar{V}_2, \quad \bar{M} = \bar{M}_2. \tag{24}$$

Substituting equations (21) and (22) into equations (17) and (18) and noting that

$$f(0,0) = 1, \qquad f(0,1) = 0, \qquad f(0,2) = 0, \qquad f(0,3) = 0 \tag{25}$$

and

$$f'(0,0) = 0, \qquad f'(0,1) = 1, \qquad f'(0,2) = 0, \qquad f'(0,3) = 0, \tag{26}$$

the following matrix relationship is obtained:

$$\begin{bmatrix} \bar{H}_1 \\ \bar{\Theta}_1 \\ \bar{H}_2 \\ \bar{\Theta}_2 \end{bmatrix} = \begin{bmatrix} 1 & 0 & 0 & 0 \\ 0 & 1 & 0 & 0 \\ b_{31} & b_{32} & b_{33} & b_{34} \\ b_{41} & b_{42} & b_{43} & b_{44} \end{bmatrix} \begin{bmatrix} C_1 \\ C_2 \\ C_3 \\ C_4 \end{bmatrix} \tag{27}$$

which may be written conveniently in the form

$$\bar{\mathbf{U}} = \mathbf{BC}, \tag{28}$$

where

$$b_{31} = f(1,0), \qquad b_{32} = f(1,1), \qquad b_{33} = f(1,2), \qquad b_{34} = f(1,3) \tag{29}$$

and

$$b_{41} = f'(1,0), \qquad b_{42} = f'(1,1), \qquad b_{43} = f'(1,2), \qquad b_{44} = f'(1,3). \tag{30}$$

Substituting equations (23) and (24) into equations (19) and (20) and noting that

$$f'''(0,0) = 0, \qquad f'''(0,1) = 0{\cdot}5v^2(1+2\rho_0)+\eta,$$
$$f'''(0,2) = 0, \qquad f'''(0,3) = 6, \qquad \beta(0) = 0{\cdot}5v^2(1+2\rho_0)+\eta \tag{31}$$

and

$$f''(0,1) = 0, \qquad f''(0,2) = 2, \qquad f''(0,3) = 0, \qquad \beta(1) = \eta, \tag{32}$$

the following matrix relationship is obtained:

$$\begin{bmatrix} \bar{V}_1 \\ \bar{M}_1 \\ \bar{V}_2 \\ \bar{M}_2 \end{bmatrix} = \begin{bmatrix} 0 & 0 & 0 & 6 \\ d_{21} & 0 & -2 & 0 \\ d_{31} & d_{32} & d_{33} & d_{34} \\ d_{41} & d_{42} & d_{43} & d_{44} \end{bmatrix} \begin{bmatrix} C_1 \\ C_2 \\ C_3 \\ C_4 \end{bmatrix} \tag{33}$$

or

$$\bar{\mathbf{F}} = \mathbf{DC}, \tag{34}$$

where

$$d_{21} = -\{0{\cdot}5v^2(1+2\rho_0)+\eta\}, \quad d_{31} = \eta f'(1,0) - f'''(1,0), \quad d_{32} = \eta f'(1,1) - f'''(1,1), \tag{35}$$

$$d_{33} = \eta f'(1,2) - f'''(1,2), \qquad d_{34} = \eta f'(1,3) - f'''(1,3) \tag{36}$$

and

$$d_{41} = f''(1,0), \qquad d_{42} = f''(1,1), \qquad d_{43} = f''(1,2), \qquad d_{44} = f''(1,3). \tag{37}$$

The dynamic stiffness matrix $\bar{\mathbf{K}}$ can be obtained by eliminating the constant vector $\mathbf{C}$ from equations (28) and (34) to give the force–displacement relationship as follows:

$$\bar{\mathbf{F}} = \bar{\mathbf{K}}\bar{\mathbf{U}} \tag{38}$$

or

$$\begin{bmatrix} \bar{V}_1 \\ \bar{M}_1 \\ \bar{V}_2 \\ \bar{M}_2 \end{bmatrix} = \begin{bmatrix} \bar{k}_{11} & \bar{k}_{12} & \bar{k}_{13} & \bar{k}_{14} \\ & \bar{k}_{22} & \bar{k}_{23} & \bar{k}_{24} \\ \textit{symmetric} & & \bar{k}_{33} & \bar{k}_{34} \\ & & & \bar{k}_{44} \end{bmatrix} \begin{bmatrix} \bar{H}_1 \\ \bar{\Theta}_1 \\ \bar{H}_2 \\ \bar{\Theta}_2 \end{bmatrix} \tag{39}$$

where

$$\bar{\mathbf{K}} = \mathbf{DB}^{-1} \tag{40}$$

is the required (non-dimensional) dynamic stiffness matrix.

Each individual element of the $\bar{\mathbf{K}}$ matrix is generated using purely algebraic method by inverting the **B** matrix algebraically and pre-multiplying the resulting matrix by the **D** matrix. The 10 independent terms of the $\bar{\mathbf{K}}$ matrix are as follows:

$$\bar{k}_{11} = 6(b_{31}b_{43} - b_{33}b_{41})/\Delta, \quad \bar{k}_{12} = 6(b_{32}b_{43} - b_{33}b_{42})/\Delta, \quad \bar{k}_{13} = -6b_{43}/\Delta, \quad \bar{k}_{14} = 6b_{33}/\Delta, \tag{41}$$

$$\bar{k}_{22} = 2(b_{32}b_{44} - b_{34}b_{44})/\Delta, \qquad \bar{k}_{23} = -2b_{44}/\Delta, \qquad \bar{k}_{24} = 2b_{34}/\Delta, \tag{42}$$

$$\bar{k}_{33} = (b_{44}d_{33} - b_{43}d_{34})/\Delta, \qquad \bar{k}_{34} = (b_{33}d_{34} - b_{34}d_{33})/\Delta, \qquad \bar{k}_{44} = (b_{33}d_{44} - b_{34}d_{43})/\Delta, \tag{43}$$

where

$$\Delta = (b_{33}b_{44} - b_{34}b_{43}). \tag{44}$$

The dynamic stiffness matrix derived above has been worked out using all parameters in non-dimensional form. The displacement, bending moment and shear force were all taken as dimensionless quantities through the use of equations (7) and (8). (Note that the slope which is the first derivative of the ordinate with respect to the abscissa remains invariant (unchanged) when X and Y co-ordinates are transformed into ξ and $\bar{h}$ by dividing with L.) The elements of the dimensional dynamic stiffness matrix **K** can now be recovered from the elements of $\bar{\mathbf{K}}$ so that

$$\begin{bmatrix} V_1 \\ M_1 \\ V_2 \\ M_2 \end{bmatrix} = \begin{bmatrix} k_{11} & k_{12} & k_{13} & k_{14} \\ & k_{22} & k_{23} & k_{24} \\ \textit{symmetric} & & k_{33} & k_{34} \\ & & & k_{44} \end{bmatrix} \begin{bmatrix} H_1 \\ \Theta_1 \\ H_2 \\ \Theta_2 \end{bmatrix}. \tag{45}$$

Using the relationships of equations (7) and (8) it can be shown easily that

$$k_{11} = W_3\bar{k}_{11}, \qquad k_{12} = W_2\bar{k}_{12}, \quad k_{13} = W_3\bar{k}_{13}, \qquad k_{14} = W_2\bar{k}_{14}, \tag{46}$$

$$k_{22} = W_1\bar{k}_{22}, \qquad k_{23} = W_2\bar{k}_{12}, \quad k_{24} = W_1\bar{k}_{24}, \tag{47}$$

$$k_{33} = W_3\bar{k}_{33}, \qquad k_{34} = W_2\bar{k}_{34}, \tag{48}$$

and

$$k_{44} = W_1\bar{k}_{44}, \tag{49}$$

where

$$W_1 = EI_{xx}/L, \qquad W_2 = EI_{xx}/L^2, \qquad W_3 = EI_{xx}/L^3 \tag{50}$$

and $\bar{k}_{11}$, $\bar{k}_{12}$, $\bar{k}_{13}$, etc., are given by equations (41)–(44).

The governing differential equation of motion for the dynamic stiffness matrix formulation of the beam referring to the in-plane motion (see XY plane in Figure 1) turns out to be similar to that of the out-of-plane motion of equation (6) except that the coefficient μ^2 appearing in the last term must be replaced by $(\mu^2 + \nu^2)$ (see reference [3], p. 623 for details). Thus, the above stiffness expressions are valid for in-plane motion of the beam provided μ^2 in equation (7) is redefined as $(\mu^2 + \nu^2)$. With this new definition of μ^2, all expressions given above will equally apply for in-plane free vibration of the beam, but, of course, the appropriate bending rigidity (EI_{zz}) for the displacement in XY plane must be used.

3. APPLICATION OF THE DYNAMIC STIFFNESS MATRIX

The above dynamic stiffness matrix can now be used to compute the natural frequencies and mode shapes of a rotating beam with various end conditions. A rotating non-uniform beam, for example a tapered beam, can also be analyzed for its free-vibration characteristics by idealizing it as an assemblage of many uniform beams, and is thus treated as a stepped beam. An accurate and reliable method of calculating the natural frequencies and mode shapes using the dynamic stiffness matrix method is to apply the well-known algorithm of Wittrick and Williams [22], which has featured literally in dozens of papers. The algorithm, unlike its proof, is very simple to use [20–21], but for a detailed insight interested readers are referred to the original work of Wittrick and Williams [22]. Basically, the algorithm needs the dynamic stiffness matrices of individual members in a structure and information about their natural frequencies when both ends are clamped. This information is needed to enable the algorithm to guarantee that no natural frequencies of the structure are missed. Thus, an explicit expression from which the clamped–clamped natural frequencies can be found facilitates an easy and straightforward application of the algorithm. Δ in equation (44) is such an expression because the clamped–clamped natural frequencies are given by its zeros. It should be noted that the actual requirement of the algorithm is to isolate these clamped–clamped natural frequencies (that is to determine how many such natural frequencies are there below a specified trial frequency) rather than actually calculating them. The Wittrick–Williams algorithm [19–22] essentially gives the number of natural frequencies of a structure that exists below an arbitrarily chosen trial frequency rather than actually calculating the natural frequencies. This simple feature of the algorithm can be exploited to advantage to enable calculation of any natural frequency of the structure to any desirable accuracy.

The above dynamic stiffness matrix can be used to solve certain specific problems (for example, the free-vibration analysis of the rotating slider mechanism shown in Figure 3 of reference [3]). However, it should be recognized that the theory has been greatly compromised because it assumes zero pre-twist of the beam axis and also zero coupling between in-plane and out-of-plane bending as well as bending and torsional motions. The theory is thus restrictive and needs further development for many practical applications such as helicopter and turbine blades for which pretwist and other coupling terms can have pronounced effects. The present paper is expected to stimulate this area of research.

4. RESULTS AND DISCUSSION

4.1. UNIFORM BEAMS

The first three dimensionless natural frequencies μ (see equation (7)) of a uniform rotating Bernoulli–Euler beam for clamped–free (C–F), clamped–clamped (C–C) clamped–pinned (C–P) and pinned–pinned (P–P) end conditions obtained from the above dynamic stiffness theory are shown in Table 1 for representative values of the non-dimensional rotation speed parameter v and hub-offset parameter r_h/L_T. Note that the first letter of the abbreviations C–F, C–C, C–P and P–P corresponds to the end condition of the left-hand end of the beam whereas the second one corresponds to that of the right-hand end. These results agree

TABLE 1

Variation of the first three dimensionless natural frequency parameter (μ) with the variations of the dimensionless angular speed (v) and hub off-set ratio (r_h/L_T)

End conditions	Natural frequency (μ)	$v = 1$		$v = 5$	
		$r_h/L_T = 0$	$r_h/L_T = 1$	$r_h/L_T = 2$	$r_h/L_T = 3$
C–F	μ_1	3·6816	3·8888	10·862	12·483
	μ_2	22·181	22·375	32·764	35·827
	μ_3	61·842	62·043	73·984	77·935
C–C	μ_1	22·465	22·601	29·866	32·101
	μ_2	61·802	61·987	72·922	76·572
	μ_3	121·04	121·25	133·81	138·23
C–P	μ_1	15·513	15·650	22·663	24·729
	μ_2	50·093	50·277	60·906	64·382
	μ_3	104·39	104·59	116·99	121·30
P–P	μ_1	10·022	10·264	19·684	22·078
	μ_2	39·642	39·889	53·132	57·235
	μ_3	88·991	89·241	103·92	108·93

completely with the exact results of reference [3] which uses a differential equation and its solution approach rather than the dynamic stiffness method. Representative results for the first three mode shapes corresponding to the above four sets of boundary conditions of the beam for values of $v = 1$ and $r_h/L_T = 1$ are shown in Figure 4. During the computation of results it has been found that the convergence of the power series method is excellent. Typically with up to 80 terms in the power series, the results obtained are accurate to six digits. When the number of terms is increased to 120 the accuracy increases to nine digits.

4.2. TAPERED BEAMS

Although any type of tapered beam can be idealized by a suitable number of uniform dynamic stiffness elements, for illustrative purposes two different types of linearly tapered cantilever beams have been chosen from the published literature [1, 14]. This has made a direct comparison of results obtained from the present theory with those available in the literature possible.

4.2.1. *Example* 1

In this example, the taper is such that the variations of the mass per unit length $m(\xi)$, and the bending rigidity $EI(\xi)$ at a (non-dimensional) distance ξ are governed by the following expressions:

$$m(\xi) = m_0(1 - c\xi) \tag{51}$$

and

$$EI(\xi) = E_0 I_0 (1 - c\xi)^3. \tag{52}$$

where m_0 and $E_0 I_0$ correspond to values of the mass per unit length and the flexural rigidity at the thick end (that is the built-in end) of the beam, respectively, and c is the taper ratio such that $0 < c < 1$. Note that equations (51) and (52) cover a wide range of cross-sections

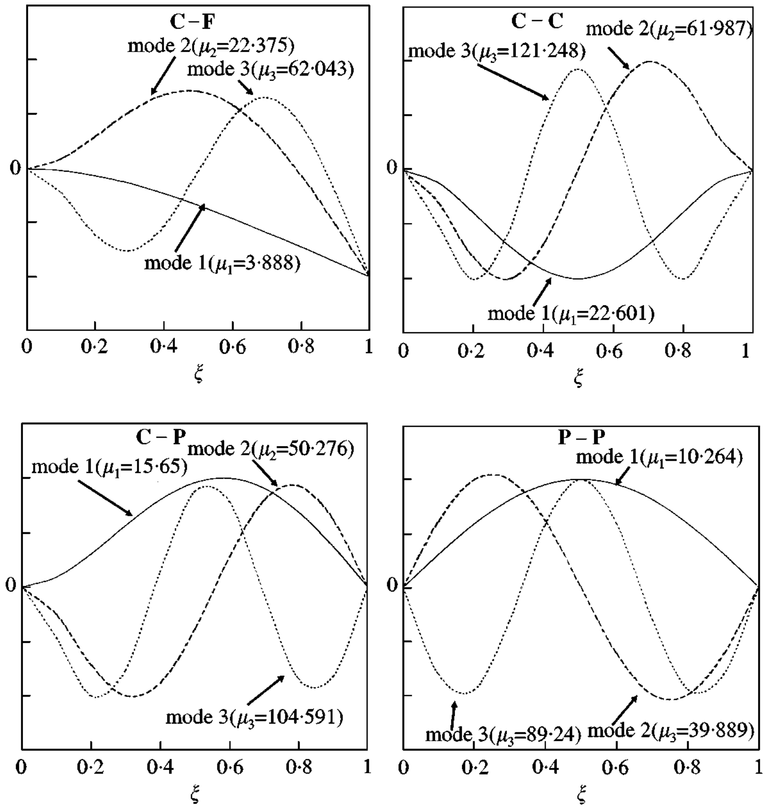

Figure 4. Mode shapes of a rotating uniform Bernoulli–Euler beam for clamped–free (C–F), clamped–clamped (C–C), clamped–pinned (C–P) and pinned–pinned (P–P) end conditions.

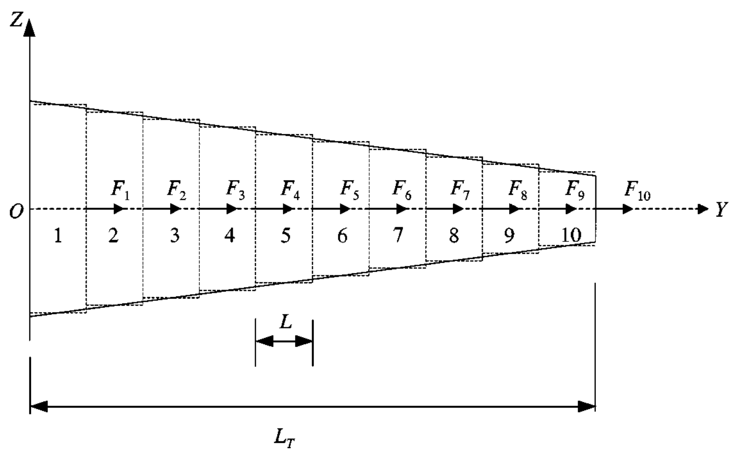

Figure 5. The idealization of a linearly tapered beam using 10 uniform elements.

for tapered beams [23] (for example, a solid rectangular cross-section with constant width and linearly varying depth).

A sketch showing a 10-element idealization of the tapered beam is given in Figure 5. The results are obtained for the case when the taper ratio is fixed at $c = 0{\cdot}5$. The data used for

TABLE 2

Data used for the 10-element idealization of the tapered beam of Example 1 with $r_h/L_T = 0$

Element no. (i)	L_i/L_T	r_i/L	m_i/m_0	$(EI)_i/E_0I_0$	$F_iL_T^2/E_0I_0$
1	0·1	0·0	0·975	0·92686	0·32888
2	0·1	0·1	0·925	0·79145	0·31500
3	0·1	0·2	0·875	0·66992	0·29313
4	0·1	0·3	0·825	0·56152	0·26425
5	0·1	0·4	0·775	0·46548	0·22938
6	0·1	0·5	0·725	0·38108	0·18950
7	0·1	0·6	0·675	0·30755	0·14563
8	0·1	0·7	0·625	0·24414	0·09875
9	0·1	0·8	0·575	0·19011	0·04988
10	0·1	0·9	0·525	0·14470	0·00000

TABLE 3

Variation of the first three non-dimensional frequency parameter (μ) of the tapered beam of Example 1 with the variation of the non-dimensional angular speed parameter (ν) for $r_h/L_T = 0$

Angular speed (ν)	Natural frequency (μ)	Present theory		Reference [14] (exact)
		10 element	20 element	
0	μ_1	3.8078	3·8198	3·8238
	μ_2	18·227	18·295	18·317
	μ_3	47·022	47·203	47·265
1	μ_1	3·9711	3·9827	3·9866
	μ_2	18·384	18·451	18·474
	μ_3	47·175	47·356	47·417
2	μ_1	4·4222	4·4331	4·4368
	μ_2	18·848	18·914	18·937
	μ_3	47·631	47·810	47·872
3	μ_1	5·0790	5·0892	5·0927
	μ_2	19·598	19·662	19·684
	μ_3	48·381	48·558	48·619
4	μ_1	5·8657	5·8755	5·8788
	μ_2	20·601	20·664	20·685
	μ_3	49·411	49·586	49·646

the 10 individual elements of Figure 5 are given in Table 2 for those readers who wish to check their own results or their computer codes based on the expressions given in this paper. Note that the dynamic stiffness method will give exact results for the stepped beam shown in Figure 5, but the results for the (actual) tapered beam will not be exact because the dynamic stiffness matrix used is not for a tapered beam. The first three non-dimensional natural frequencies (μ) for a range of non-dimensional rotational speed parameters (ν) obtained using the dynamic stiffness theory when the hub offset ratio r_h/L_T is equal to zero, are given in Table 3 for 10- and 20-element idealization respectively. The authors of reference [14] have reported exact results for this particular example although their main investigation is based on approximate theory using the finite element method. These results are also shown in Table 3 for comparison. The agreement with exact results particularly

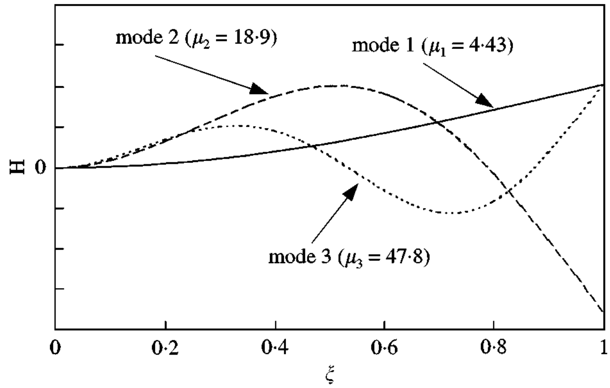

Figure 6. Mode shapes of the rotating tapered cantilever beam of Example 1.

TABLE 4

Variation of the first three non-dimensional frequency parameter (μ) *of the tapered beam of Example* 1 *with the variation of the non-dimensional angular speed parameter* (v) *for* $r_h/L_T = 1$

Angular speed (v)	Natural frequency (μ)	Present theory		
		10 elements	20 elements	40 elements
1	μ_1	4·3719	4·3830	4·3858
	μ_2	18·791	18·857	18·874
	μ_3	47·590	47·769	47·815
2	μ_1	5·7291	5·7392	5·7417
	μ_2	20·388	20·452	20·468
	μ_3	49·250	49·426	49·472
3	μ_1	7·4394	7·4494	7·4519
	μ_2	22·799	22·859	22·874
	μ_3	51·891	52·062	52·106
4	μ_1	9·2964	9·3068	9·3094
	μ_2	25·789	25·847	25·861
	μ_3	55·359	55·525	55·567

with 20-element idealization is quite good as can be seen. The first three modes for this cantilever beam obtained from the present theory when using 20 elements are shown in Figure 6 for the case when the rotational speed parameter v was set to 2.

The next set of results for this example is obtained when the hub offset ratio r_h/L_T is non-zero and fixed at 2. The first three non-dimensional natural frequencies for a wide range of angular speed, obtained from 10-, 20- and 40-element idealization are shown in Table 4. The rapid convergence of results with increasing number of elements is evident from these results.

4.2.2. *Example* 2

The second example used to obtain numerical results is that of Wright *et al.* [1]. For this particular problem the taper is such that both the mass per unit length $m(\xi)$, and the bending rigidity $EI(\xi)$ vary linearly along the length of the beam so that

$$m(\xi) = m_0(1 - c_1\xi) \tag{53}$$

TABLE 5

Variation of the first three non-dimensional frequency parameter (μ) of the tapered beam of Example 2 with the variation of the non-dimensional angular speed parameter (ν) and the hub-offset ratio parameter (r_h/L_T)

Hub offset ratio (r_h/L_T)	Angular speed (ν)	Natural frequency (μ)	Present theory 20 elements	Present theory 50 elements	Exact (Reference [1])
0	0	μ_1	5·2656	5·2725	5·2738
		μ_2	23·949	23·995	24·004
		μ_3	59·800	59·943	59·970
	5	μ_1	7·6382	7·6434	7·6443
		μ_2	26·407	26·450	26·458
		μ_3	62·240	62·380	62·407
1	1	μ_1	5·5427	5·5493	5·5507
		μ_2	24·195	24·241	24·250
		μ_3	60·043	60·186	60·214
	5	μ_1	10·076	10·082	10·083
		μ_2	29·484	29·525	29·535
		μ_3	65·599	65·737	67·765
5	1	μ_1	6·1418	6·1482	6·1494
		μ_2	24·759	24·804	24·813
		μ_3	60·615	60·758	60·785
	5	μ_1	16·504	16·510	16·512
		μ_2	39·362	39·404	39·413
		μ_3	77·439	77·575	77·602

and

$$EI(\xi) = E_0 I_0 (1 - c_2 \xi), \tag{54}$$

where m_0 and E_0I_0 correspond to values of the mass per unit length and the flexural rigidity at the thick end of the beam, respectively, and c_1 and c_2 are the proportionality constants.

Proceeding in the same way as in Example 1, the results are obtained for cantilever end condition of the tapered beam using a stepped beam representation. Representative results for the first three non-dimensional natural frequencies for a range of hub-offset ratios and angular speeds, when using 20- and 50-element idealization are shown in Table 5 alongside the exact result obtained from reference [1]. The constants c_1 and c_2 of equations (53) and (54) were set to 0·8 and 0·95, respectively, so that a direct comparison of results with those of reference [1] is possible. The agreement with the exact result, particularly when using the present theory with 50 elements is excellent (the discrepancy is less than 0·05%) as can be seen.

4.3. FURTHER INSIGHTS INTO THE RESULTS OF TAPERED BEAMS

The results for the tapered beams of Examples 1 and 2 shown in Tables 3–5 indicate that a stepped representation of a linearly tapered beam using uniform dynamic stiffness elements, gives a lower bound on natural frequencies. This is to be expected because when a tapered element is represented by a series of uniform elements, the stiffness properties are underestimated [23] by such idealization whereas the mass of the element remains invariant. As a consequence a reduction in natural frequencies is expected to occur.

The results of Tables 3–5 indicate that with a discrete element idealization, the accuracy of natural frequencies improves when the hub-offset ratio or angular speed increases. The reason for this can be attributed to the fact that for higher hub-offset ratios or angular speeds, the centrifugal force terms dominate the (mechanical) bending stiffness terms, and noting that the centrifugal terms are better represented by stepped approximation than the bending stiffness terms. This accords with similar findings of a recently published paper [24].

The convergence of results with number of elements (used to approximate the taper) was studied for both examples. Figure 7 shows the variation of percentage error with number of elements (N) for the fundamental natural frequency of the two beams, respectively, for two representative sets of values of hub-offset ratios and angular speeds. The accuracy increases with the number of elements as expected and the results show that only as few as 10 (uniform) elements can give acceptable (engineering) accuracy in the fundamental natural frequency when idealizing the tapered beam, the errors being less than 0·5%. Further studies of convergence and accuracy of results were carried out to assess the computational efficiency of the proposed method.

The investigation revealed that in order to obtain five-figure accuracy in natural frequencies, around 200 uniform elements will be required to idealize a tapered beam of the type under consideration. As the computer time increases with the number of elements, and hence with the accuracy, estimates of the CPU time on a Sun (Ultra-2) workstation was taken when locating the first three natural frequencies of the two example beams. In each run, a data-specifiable convergence criterion CV was satisfied where the computational accuracy of the results was 1 part in CV. For example, if CV is set to 10^6 the accuracy obtained will be 1 part in a million. The plot of the elapsed CPU time against the convergence criteria CV when locating the first and third natural frequencies of the first example beam is shown in Figure 8. Similar trends were observed for the second example but are not shown here for brevity. The rapid growth of the CPU time with accuracy, particularly for higher natural frequencies is noticeable.

The results shown in Figures 7 and 8 prompted a further study to investigate whether or not it is possible to extrapolate accurate results for the natural frequencies of tapered beams from the approximate results obtained using relatively smaller number of uniform elements.

The results shown in Figure 7 indicate that the natural frequencies converge almost parabolically with the number of elements (N). This trend was further confirmed by a number of case studies. These numerical studies suggest that the exact result can be related to the approximate result and the number of elements by fitting a curve which is that of a parabola. Thus if f_E is the exact natural frequency of a tapered beam and f_N is the approximate natural frequency obtained by using N number of uniform elements, the following relationship is taken to be valid:

$$f_N = f_E(1 - K/N^2). \tag{55}$$

where K is a constant.

If the approximate natural frequency is obtained by using, respectively, N_1 and N_2 number of elements ($N_2 > N_1$), it can be shown with the help of equation (55), that the exact natural frequencies can be established as the parabolic limit of the two discrete element idealization results, as follows:

$$f_E = f_{N_2} + \frac{(N_1)^2}{(N_2)^2 - (N_1)^2}(f_{N_2} - f_{N_1}), \tag{56}$$

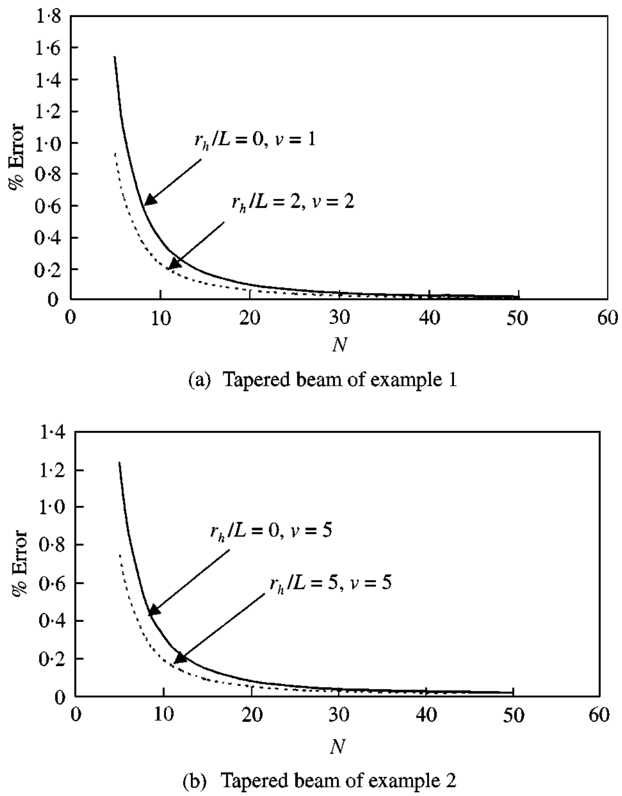

Figure 7. Variation of percentage error with number of elements for the fundamental natural frequency of tapered beams.

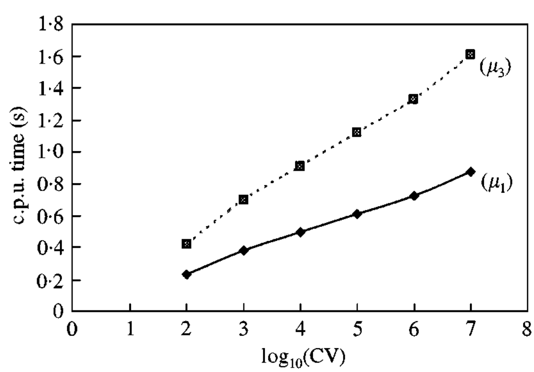

Figure 8. Variation of CPU time with convergence criteria CV (accuracy is 1 part in CV) for the first and third natural frequency of the tapered beam of Example 1.

where f_{N_1} and f_{N_2} are the natural frequencies corresponding to N_1 and N_2 element idealization of the tapered beam.

With the help of equation (56) the parabolic limits of the first three natural frequencies of the two example (tapered) beams were established using, respectively, 10 and 20 elements (see Table 3) for Example 1, and 20 and 50 elements for Example 2 (see Table 5). These results are shown in Table 6 for the case when the hub-offset ratio is set to zero. For

TABLE 6

Extrapolation of natural frequencies of tapered beams using the parabolic limit when $r_h/L_T = 0$

Anglar speed (v)	Natural frequency (μ)	Example 1: Parabolic limit using 10 and 20 elements	Example 2: Parabolic limit using 20 and 50 elements
0	μ_1	3·8238	5·2738
	μ_2	18·318	24·004
	μ_3	47·263	59·970
1	μ_1	3·9866	5·3903
	μ_2	18·473	24·107
	μ_3	47·416	60·069
2	μ_1	4·4367	5·7249
	μ_2	18·936	24·413
	μ_3	47·870	60·367
3	μ_1	5·0926	6·2402
	μ_2	19·683	24·915
	μ_3	48·617	60·859
4	μ_1	5·8788	6·8928
	μ_2	20·685	25·601
	μ_3	49·644	61·541

Example 1, the results obtained using the parabolic limit are well within 0·005% of the exact results whereas for Example 2, the results agreed to full five figures of the exact results quoted in the literature. The procedure shows that very substantial saving in computer time can be made and at the same time sufficient accuracy can be retained when predicting the free-vibration characteristics of rotating tapered beams using uniform dynamic stiffness elements.

5. CONCLUSIONS

A dynamic stiffness matrix has been developed for the first time for a rotating Bernoulli–Euler beam using the Frobenius method of solution of the governing differential equation in power series. The application of the dynamic stiffness matrix with particular reference to the Wittrick–Williams algorithm is demonstrated by numerical results. The theory developed gives exact natural frequencies (up to machine accuracy) for rotating uniform beams, but is fairly general to account for the free-vibration characteristics of rotating non-uniform beams in a sufficiently accurate manner. Using the proposed theory, different sets of results for uniform and tapered beams are given which show very good agreement with published results. It has been shown that when idealizing a tapered beam by using a number of uniform dynamic stiffness element, the parabolic limit of the approximate results gives an accurate estimate of the exact result. The research reported in this paper is expected to stimulate further research on dynamic stiffness formulation of complex rotating structural systems.

REFERENCES

1. A. WRIGHT, C. SMITH, R. THRESHER and J. WANG 1982 *Journal of Applied Mechanics* **49**, 197–202. Vibration modes of centrifugally stiffened beams.

2. D. STORTI and Y. ABOELNAGA 1987 *Journal of Applied Mechanics* **54**, 311–314. Bending vibration of a class of rotating beams with hypergeometric solutions.
3. S. NAGULESWARAN 1994 *Journal of Sound and Vibration* **176**, 613–624. Lateral vibration of a centrifugally tensioned uniform Euler–Bernoulli beam.
4. S. NAGULESWARAN 1997 *Journal of Sound and Vibration* **200**, 63–81. Out-of-plane vibration of a uniform Euler–Bernoulli beam attached to the inside of a rotating rim.
5. M. SCHILHANSL 1958 *Transactions of ASME, Journal of Applied Mechanics* **25**, 28–30. Bending frequencies of a rotating cantilever beam.
6. C. H. J. FOX and J. S. BURDESS 1979 *Journal of Sound and Vibration* **65**, 151–158. The natural frequencies of a thin rotating cantilever with offset root.
7. H. H. YOO and S. H. SHIN 1998 *Journal of Sound and Vibration* **212**, 807–828. Vibration analysis of rotating cantilever beams.
8. W. E. BOYCE 1956 *Transactions of ASME, Journal of Applied Mechanics* **23**, 287–290. Effect of hub radius on the vibration of uniform bar.
9. D. PNUELI 1972 *Transactions of ASME, Journal of Applied Mechanics* **39**, 602–604. Natural bending frequency comparable to rotational frequency in rotating cantilever beam.
10. H. LO, J. E. GOLDBERG and J. L. BOGDANOFF 1960 *Transactions of ASME, Journal of Applied Mechanics* **27**, 548–550. Effect of small hub-radius change on bending frequencies of a rotating beam.
11. L. H. JONES 1975 *Quarterly of Applied Mathematics* **33**, 193–203. The transverse vibration of a rotating beam with tip mass: the method of integral equations.
12. V. T. NAGARAJ and P. SHANTHAKUMAR 1975 *Journal of Sound and Vibration* **43**, 575–577. Rotor blade vibrations by the Galerkin finite element method.
13. S. PUTTER and H. MANOR 1978 *Journal of Sound and Vibration* **56**, 175–185. Natural frequencies of radial rotating beams.
14. D. H. HODGES and M. J. RUTKOWSKI 1981 *American Institute of Aeronautics and Astronautics Journal* **19**, 1459–1466. Free vibration analysis of rotating beams by a variable order finite element method.
15. K. M. UDUPA and T. K. VARADAN 1990 *Journal of Sound and Vibration* **138**, 447–456. Hierarchical finite element method for rotating beams.
16. A. BAZOUNE, Y. A. KHULIEF and N. G. STEPHEN 1999 *Journal of Sound and Vibration* **219**, 157–174. Further results for modal characteristics of rotating tapered Timoshenko beams.
17. R. O. STAFFORD and V. GIURGIUTIU 1975 *International Journal of Mechanical Sciences* **17**, 719–727. Semi-analytic methods for rotating Timoshenko beams.
18. V. GIURGIUTIU and R. O. STAFFORD 1977 *Vertica* **1**, 291–306. Semi-analytic methods for frequencies and mode shapes of rotor blades.
19. J. R. BANERJEE 1997 *Computers and Structures* **63**, 101–103. Dynamic stiffness formulation for structural elements: a general approach.
20. F. W. WILLIAMS and W. H. WITTRICK 1983 *ASCE Journal of Structural Engineering* **109**, 169–187. Exact buckling and frequency calculations surveyed.
21. F. W. WILLIAMS 1993 *Computer and Structures* **48**, 547–552. Review of exact buckling and frequency calculations with optional multi-level substructuring.
22. W. H. WITTRICK and F. W. WILLIAMS 1971 *Quarterly Journal of Mechanics and Applied Mathematics* **24**, 263–284. A general algorithm for computing natural frequencies of elastic structures.
23. J. R. BANERJEE and F. W. WILLIAMS 1986 *International Journal for Numerical Methods in Engineering* **23**, 1615–1628. Exact Bernoulli–Euler static stiffness matrix for a range of tapered beam columns.
24. S. M. HASHEMI, M. J. RICHARD and G. DHATT 1999 *Journal of Sound and Vibration* **220**, 601–624. A new dynamic finite element (DFE) formulation for lateral free vibration of Euler–Bernoulli spinning beams using trigonometric shape functions.